

## Studies of the crystal structure and crystal chemistry of titanomaghemite

S. COLLYER

Department of Geological Sciences, Aston University, Aston Triangle, Birmingham B4 7ET, England

N. W. GRIMES

Department of Applied Physics, Aston University, Aston Triangle, Birmingham B4 7ET, England

D. J. VAUGHAN

Department of Geology, University of Manchester, Manchester M13 9PL, England

G. LONGWORTH

Nuclear Physics Division, Atomic Energy Research Establishment, Harwell, Didcot, Oxfordshire OX11 0RA, England

### ABSTRACT

A natural single crystal of titanomaghemite from Pretoria, South Africa, containing 8.62 wt% Ti and 54.36 wt% Fe as determined by electron-microprobe analysis, has been studied by X-ray diffraction and Mössbauer spectroscopy. A crystal-structure parameter refinement of this titanomaghemite was undertaken, and values for the atom positions, anisotropic thermal parameters, and bond lengths are reported ( $R = 0.0235$ ). The lattice is primitive cubic ( $a = 8.341(1) \text{ \AA}$ ) with space group  $P4_332$  (or the enantiomorphous  $P4_332$ ). Studies of this sample, and of two powder samples of synthetic end-member maghemite, using  $^{57}\text{Fe}$  Mössbauer spectroscopy at 300 K and 4.2 K and in a longitudinal applied magnetic field of 4.2 T, indicate that for the end-member  $\gamma\text{-Fe}_2\text{O}_3$  samples, cation vacancies are restricted to octahedral sites. Combined single-crystal X-ray studies and Mössbauer spectroscopy of the titanomaghemite have given the following structural formula:



where  $\square$  represents a cation vacancy. As the above formula shows, there are cation vacancies on both tetrahedral and octahedral sites in this titanomaghemite, the majority being on the octahedral sites. We believe the evidence of the Mössbauer spectra points to  $\text{Fe}^{2+}$  on the octahedral site. Mössbauer parameters are reported for the end-member  $\gamma\text{-Fe}_2\text{O}_3$  samples and the titanomaghemite, and the cation and vacancy distributions on the sites in the latter are discussed in the light of previously published models.

### INTRODUCTION

Maghemite,  $\gamma\text{-Fe}_2\text{O}_3$ , was first reported as a natural species by Sosman and Posnjak (1925), who also noted the similarity of its X-ray powder-diffraction pattern to that of magnetite. It soon became evident that maghemite occurs in nature as a low-temperature oxidation product of magnetite and that it can be produced in the laboratory by magnetite oxidation. Many natural magnetites contain significant amounts of Ti, and these titanomagnetites may undergo oxidation to form titanomaghemites. In the titanomaghemites, therefore, both Fe = Ti substitution and the substitution of vacancies for Fe atoms occurs.

Uncertainty remains as to the precise symmetry and structure of end-member maghemite and as to the structure and cation and vacancy distributions in titanomaghemites. Notable among more recent studies is that of Smith (1979), undertaken on natural material using electron diffraction. Here the structure was found to be similar to that of ordered lithium ferrite ( $\text{LiFe}_3\text{O}_8$ ) as deter-

mined by Braun (1952), with the vacancies taking the place of the Li atoms; the space group was found to be one of the enantiomorphous pair  $P4_332$ - $P4_332$ . In the present work, Mössbauer studies of end-member maghemites and a titanomaghemite, along with a structure parameter refinement using new X-ray diffraction data from the titanomaghemite are reported. The results are discussed with reference to proposed models for the cation distribution in titanomaghemites.

Bauminger et al. (1961) and Kelly et al. (1961) made the first  $^{57}\text{Fe}$  Mössbauer studies of  $\gamma\text{-Fe}_2\text{O}_3$ . They found that the subspectra produced by  $\text{Fe}^{3+}$  on tetrahedral and octahedral sites completely overlap at room temperature, giving a single six-peak hyperfine pattern. Armstrong et al. (1966) demonstrated that it is possible to separate these two sublattice contributions by the application of an external magnetic field. From the intensity ratio between the two subspectra, they estimated the numbers of Fe atoms on octahedral and tetrahedral sites and suggested that the vacancies are restricted to octahedral sites.

### SAMPLE MATERIAL

A natural specimen of "maghemite" was obtained from the British Museum (Natural History). This sample (BM1929,1687), from Pretoria, South Africa, appeared to contain some relatively pure, single crystals of maghemite and to be ideally suited for detailed study.

In addition, two finely powdered samples of synthetic  $\gamma$ -Fe<sub>2</sub>O<sub>3</sub> (samples M1 and M2) were available for comparative studies. These samples had been used in previous studies by other workers (Greaves, 1983; Cormack and Price, 1985) and were, therefore, reasonably well characterized.

### EXPERIMENTAL PROCEDURES

Specimen BM1929,1687 was made up of a number of grains, several of which were mounted and polished for examination using reflected-light microscopy. Standard techniques were employed (as described in Craig and Vaughan, 1981). This material was also analyzed using the electron microprobe. A Cambridge Microscan 5 instrument operating at 15-kV accelerating voltage was used: pure Fe, Cr, and Ti metals, and pure synthetic Al<sub>2</sub>O<sub>3</sub>, MgO, Mn<sub>2</sub>O<sub>4</sub>, and CaSiO<sub>3</sub> were employed as standards, and the raw data were corrected by using the procedures described by Sweatman and Long (1969).

The Mössbauer effect in Fe (<sup>57</sup>Fe) was studied in all samples. The equipment used consisted of the Harwell spectrometer drive and counter systems coupled to the Ino-Tech 5200 multichannel analyzer utilizing 512 channels for data collection. The  $\gamma$ -ray source was <sup>57</sup>Co in a Rh matrix. Fe foil was used in calibration, and all isomer shifts are quoted relative to the center of gravity of the spectrum of pure Fe as zero velocity. Computer fitting of spectra was undertaken using the procedures described by Longworth (1984). Specimens were powders (prepared by grinding under acetone where necessary), spread out to a disc of thickness such that the average sample concentration was 25 mg·cm<sup>-2</sup>.

A fragment of specimen BM1929,1687 was ground into a sphere of radius 0.20(5) mm using an air-driven grinder based on that described by Bond (1951). This spherical fragment was then mounted on an Enraf-Nonius CAD-4 automated diffractometer, and integrated X-ray intensities were collected at room temperature, employing the  $\omega$ - $2\theta$  scan technique. The radiation used was MoK $\alpha$  ( $\lambda = 0.71069$  Å), monochromatized after reflection by pyrolytic graphite with a monochromator angle  $\theta_m = 6.05^\circ$ . The X-ray tube was operated at 40 kV and 20 mA. As further discussed below, these X-ray data were used for a crystal-structure parameter refinement employing the crystallographic least-squares program CRYLSQ from the software package X-RAY74 (Stewart et al., 1974).

### RESULTS

#### Composition of specimen BM1929,1687

Examination of a bulk section of specimen BM1929,1687 using reflected light microscopy showed it to be essentially homogeneous, although in some areas a small amount (~4%) of an additional phase was observed. Unlike the maghemite, which is isotropic, this brownish-gray phase was strongly anisotropic and exhibited weak reflection pleochroism. These properties are characteristic of ilmenite, an identification confirmed by electron-microprobe analysis. Electron-microprobe anal-

ysis of the major phase that makes up specimen BM1929,1687 confirmed that it was essentially homogeneous and contained, in addition to oxygen, detectable amounts of Fe and Ti. The elements Si, Al, Mg, Ca, Cr, and Mn were checked for but not detected. An average of 10 spot analyses gave a composition of 54.36 wt% Fe and 8.82 wt% Ti; the specimen was therefore identified as a titanomaghemite.

#### Mössbauer data

Mössbauer spectra of maghemite specimens M1 and M2 were obtained at room temperature and also at 4.2 K in a longitudinal magnetic field of 4.2 T. The room-temperature spectrum of specimen M1 is shown in Figure 1. The spectra of both M1 and M2 are made up essentially of two six-peak hyperfine patterns, arising from Fe on tetrahedral and octahedral sites in the structure. There is also a third six-peak subspectrum of very low intensity (~4% of the total area) with parameters showing it is a small amount of  $\alpha$ -Fe<sub>2</sub>O<sub>3</sub> impurity. The Mössbauer parameters (Table 1) show that all of the Fe is present as Fe<sup>3+</sup>; these parameters are in reasonable agreement with the results of previous workers (see Table 1). The goodness of fit ( $\chi^2$ ) value was 1.5 for the spectrum of M1 (Fig. 1) and 1.0 for M2. However, the resolution of contributions from A and B sites was not adequate to have much confidence in relative areas obtained.

In order to improve the resolution of the subspectra due to Fe<sup>3+</sup> on tetrahedral and octahedral sites, spectra were recorded for specimens M1 and M2 at 4.2 K in a longitudinal magnetic field of 4.2 T. The two major hyperfine patterns clearly seen in Figure 2 indicate the presence of two magnetic substructures with antiparallel spins. The Mössbauer parameters for the two subspectra are presented in Table 1; assignment of these subspectra to Fe<sup>3+</sup> on octahedral and tetrahedral sites was possible because the (outer) peaks arising from the minority (tetrahedral) site are clearly of lower intensity. The goodness of fit ( $\chi^2$ ) for the spectrum of specimen M1 shown in Figure 2 was 1.8, and that of specimen M2 was 1.0.

Site occupancies of the Fe atoms in maghemite may be determined from the areas under the Mössbauer peaks, provided that (as here) the absorber is thin, the temperature is low, and the recoil-free fractions of Fe on tetrahedral and octahedral sites are equal. The last assumption was experimentally investigated by Sawatzky et al. (1969), who studied the recoil-free fraction of Fe in tetrahedral and octahedral sites in the spinel structure and found a ratio for tetrahedral to octahedral sites of 0.94(2) at room temperature and 0.99(1) at near absolute zero. Thus, at low temperature, the recoil-free fractions from Fe<sup>3+</sup> on tetrahedral and octahedral sites can be assumed to be equal, and peak intensities can be used to estimate the ratio of Fe<sup>3+</sup> ions on tetrahedral and octahedral sites (Table 1). For M1 and M2, this ratio is found to be 0.65(5). If all of the vacancies are located on octahedral sites, this value would be 0.6; if all are located on tetrahedral sites, the ratio would be 0.33, and if the vacancies are equally

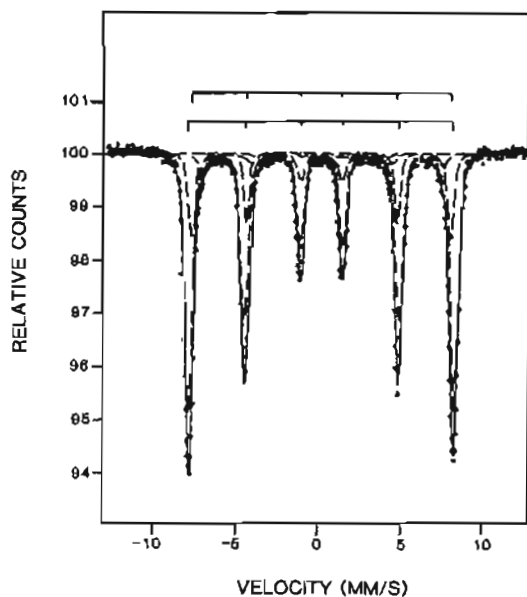


Fig. 1. Mössbauer spectrum of maghemite specimen M1 at room temperature. In this figure and Figs. 2, 3, and 4, the solid lines represent least-squares fits of data points to superimposed Lorentzian curves (shown dashed), and the zero of the velocity scale is the center of gravity of the spectrum of Fe foil at room temperature.

distributed between the two sites, then the ratio would be 0.5. The result found here suggests that, within experimental error, the cation vacancies in maghemite specimens M1 and M2 are restricted to octahedral sites.

The titanomaghemite specimen (BM1929,1687) was also studied at room temperature and at 4.2 K in a longitudinal magnetic field of 4.2 T, and the spectra are shown in Figures 3 and 4. The room-temperature spectrum (Fig.

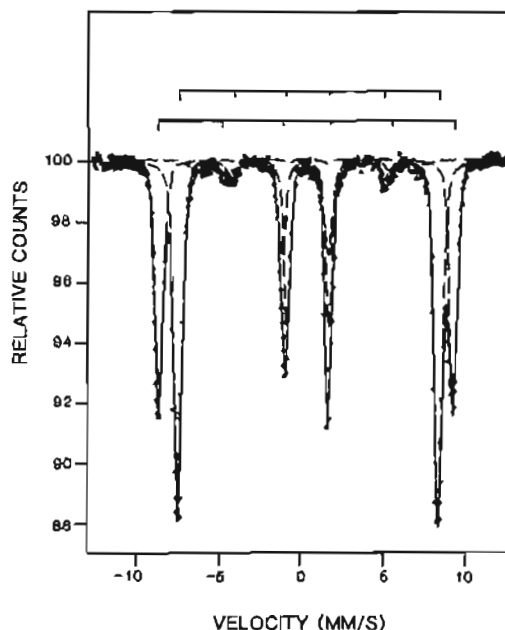


Fig. 2. Mössbauer spectrum of maghemite specimen M1 at 4.2 K in a longitudinal magnetic field of 4.2 T.

3) can be fitted to three six-peak hyperfine patterns along with two quadrupole doublets. The first of these doublets has an isomer shift of  $1.063(5) \text{ mm} \cdot \text{s}^{-1}$  and a quadrupole splitting of  $0.476(5) \text{ mm} \cdot \text{s}^{-1}$ ; the second has an isomer shift of  $0.365(5) \text{ mm} \cdot \text{s}^{-1}$  and quadrupole splitting of  $0.360(5) \text{ mm} \cdot \text{s}^{-1}$ . These parameters, in conjunction with the optical and analytical data mentioned above, enable these features to be assigned to a small amount of hemilmenite impurity, i.e., to a phase of composition  $(1-x) \text{FeTiO}_3 \cdot x \text{Fe}_2\text{O}_3$  containing both  $\text{Fe}^{2+}$  and  $\text{Fe}^{3+}$  ions. The Mössbauer parameters of three hyperfine patterns re-

TABLE 1. Mössbauer parameters for maghemite specimens M1 and M2 along with the data of previous workers

Site and ion	Temp (K)	Hyperfine field (kOe)	Isomer shift ( $\text{mm} \cdot \text{s}^{-1}$ )	Quadrupole splitting ( $\text{mm} \cdot \text{s}^{-1}$ )	Relative area (%)	Reference
A and B	300	505(20)	0.31(5)	—	—	Bauminger et al. (1961)
A and B	300	496(20)	0.32(9)	—	—	Kelly et al. (1961)
A	300	499	0.35	—	—	Coey et al. (1971)
B		505	0.46	—	—	
A	4.2	488(5)	0.36(4)	—	—	Armstrong et al. (1986)
B		499(5)	0.50(4)	—	—	
Specimen M1						
A ( $\text{Fe}^{3+}$ )	300	488(5)	0.304(5)	-0.011(5)	23 (normalized)	This work
B ( $\text{Fe}^{3+}$ )	300	501(5)	0.324(5)	0.008(5)	77	
Specimen M1 in a field of 4.2 T						
A ( $\text{Fe}^{3+}$ )	4.2	553(5)	0.348(5)	0.015(5)	40	This work
B ( $\text{Fe}^{3+}$ )	4.2	490(5)	0.489(5)	-0.000(5)	60	
Specimen M2						
A ( $\text{Fe}^{3+}$ )	300	498(5)	0.281(5)	-0.002(5)	25 (normalized)	This work
B ( $\text{Fe}^{3+}$ )	300	504(5)	0.338(5)	-0.021(5)	74	
Specimen M2 in a field of 4.2 T						
A ( $\text{Fe}^{3+}$ )	4.2	554(5)	0.356(5)	0.003(5)	39	This work
B ( $\text{Fe}^{3+}$ )	4.2	491(5)	0.487(5)	0.002(5)	61	

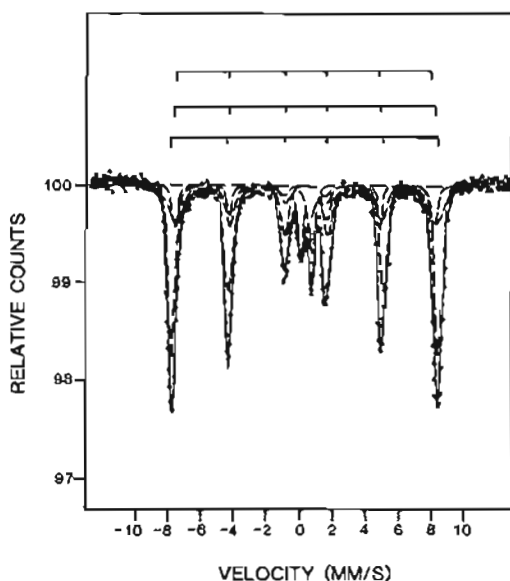


Fig. 3. Mössbauer spectrum of titanomaghemite specimen BM1929,1687 at room temperature.

remaining after removal of these impurity peaks, and hence attributable to the titanomaghemite, are given in Table 2. Such broad Mössbauer lines are hard to fit uniquely, and initially attempts were made to fit Lorentzian lines in the usual way; these values are shown first in Table 2.

TABLE 2. Mössbauer parameters for maghemite specimen BM1929,1687 with cation distribution and structural formula

Site and ion	Temp (K)	Hyperfine field (kOe)	Isomer shift (mm·s <sup>-1</sup> )	Quadrupole splitting (mm·s <sup>-1</sup> )	Relative area (%)
A (Fe <sup>3+</sup> )	300	491(5) [489]	0.352(5) [0.304]	-0.003(5) [0.304]	26
B (Fe <sup>3+</sup> )		504(5) [505]	0.338(5) [0.341]	-0.021(5) [0.341]	60
B (Fe <sup>2+</sup> )		489(5) [455]	0.281(5) [0.496]	-0.002(5) [0.496]	14
In an external field of 4.2 T					
A (Fe <sup>3+</sup> )	4.2	551(5) [551]	0.364(5) [0.382]	0.012(5) [0.382]	41
B (Fe <sup>3+</sup> )		492(5) [492]	0.514(5) [0.501]	-0.028(5) [0.501]	48
B (Fe <sup>2+</sup> )		433(5) [433]	0.406(5) [0.508]	0.069(5) [0.508]	11

Oxide	Wt%	No. of ions in formula (32 oxygens/unit cell)
Fe <sub>2</sub> O <sub>3</sub> (tet.)	34.49	7.78
Fe <sub>2</sub> O <sub>3</sub> (oct.)	35.06	7.81
FeO (oct.)	7.36	1.84
TiO <sub>2</sub> (oct.)	14.71	3.32

Number of cation vacancies by difference = 3.15; hence the structural formula is



where  $\square$  = vacancy.

Note: Parameters in square brackets refer to alternative fitting using a Gaussian distribution of Lorentzian lines; see text for discussion.

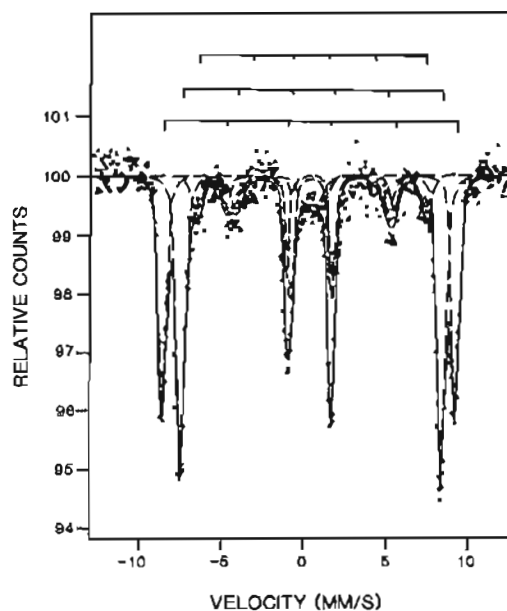


Fig. 4. Mössbauer spectrum of titanomaghemite specimen BM1929,1687 at 4.2 K in a longitudinal magnetic field of 4.2 T.

However, it was felt that a more realistic approach was to use a Gaussian distribution of Lorentzian lines (Voigt particles) as would be expected where the hyperfine field is disturbed in a random fashion as in a vacancy-containing phase such as maghemite. The values obtained in this way are also shown in Table 2 (in square brackets). The first two subspectra listed are interpreted as arising from Fe<sup>2+</sup> ions in tetrahedral (A site) and octahedral (B site) coordination and have hyperfine fields and isomer shifts consistent with this interpretation. The third subspectrum is interpreted as arising from Fe<sup>2+</sup> on the octahedral sites, chiefly on the basis of the hyperfine field (455 kOe) that is a more reliably determinable parameter in such complex spectra. Although the evidence for Fe<sup>2+</sup> is not conclusive, we believe this to be the most reasonable interpretation of the data.

In order to improve resolution of the tetrahedral- and octahedral-site subspectra and determine site populations in this specimen with reasonable accuracy, the spectrum was again recorded at 4.2 K in an external field (Fig. 4). Fitting of this spectrum to Lorentzian lines gave the parameters in Table 2 with a  $\chi^2$  value of 1.1. Again, somewhat different parameters were obtained using the alternative method of fitting (Voigt particles) and accord with our assignment of tetrahedral- and octahedral-site Fe<sup>3+</sup> and octahedral-site Fe<sup>2+</sup>; these values are given in square brackets in Table 2. However, the relative areas obtained for the three subspectra did not differ significantly regardless of the method of fitting. In order to propose a cation-distribution model for the specimen, it was necessary to assume that all of the Ti<sup>4+</sup> occurs on octahedral sites. This assumption is in agreement with neutron-diffraction studies (e.g., Ishikawa et al., 1971), magnetic

measurements (O'Reilly and Banerjee, 1965; Stephenson, 1969), and the theoretical models discussed elsewhere in this paper, all of which indicate that  $Ti^{4+}$  occupies only octahedral sites in titanomagnetites and titanomaghemites. Initially, it was also assumed that the amount of  $Fe^{3+}$  occupying tetrahedral sites is the same as in end-member maghemite (i.e., 24.12 wt%), a reasonable first approximation since the relative areas of tetrahedral-site subspectra, after removal of impurity peaks, for maghemite specimen M1 of 39.53 and specimen M2 of 39.43 both agree, within experimental error, with that of 40.38 found for titanomaghemite BM1929.1687. The remaining Fe (determined from microprobe analysis) was then assigned to the octahedral site and divided between  $Fe^{2+}$  and  $Fe^{3+}$  in the ratio 48.35:11.27, given by the relative areas of the relevant peaks in the Mössbauer spectra. By this procedure, as summarized in Table 2, a structural formula for this titanomaghemite specimen was calculated.

#### X-ray data

A preliminary examination of titanomaghemite specimen BM1929.1687 using the CAD-4 diffractometer indicated that the Bravais lattice is primitive cubic and the reflections observed are consistent with the space group  $P4_32$  (or  $P4_32$ ). No reflections of the type  $\{h00\}$  with  $h = 2n$ , e.g., 002 and 006, were observed; and the alternative space group  $P2_13$  was immediately ruled out. The space group  $P4_32$  was therefore used in a crystal-structure refinement employing the X-ray intensity data collected from this specimen.

All reflections in one hemisphere of reciprocal space out to an angle of  $\theta = 30^\circ$  were collected, using a scan time of  $3.33 \text{ deg} \cdot \text{min}^{-1}$ , giving a total of 3543 non-Friedel related reflections. Under  $P4_32$  symmetry, reflections of the type  $\{h00\}$  with  $h = 2n$  are systematically absent; these reflections were still measured as a check to ensure that they really are of zero intensity. In fact, reflections of this type were found to be absent.

During data collection, intensity control was maintained using the reflections  $\bar{5}11$ ,  $\bar{5}33$ , and  $\bar{8}44$ , and orientation control using  $\bar{4}44$ ,  $\bar{7}13$ , and  $\bar{8}44$ . After measuring every 200 reflections, the diffractometer returned and measured the intensity of the three intensity-control reflections. Any fall-off in the intensity of these standards detected was then employed to correct all intensities, using linear interpolation to the control reflections. The three orientation-control reflections were measured every 7200 s of X-ray exposure time and allowed the diffractometer to check the crystal orientation, and if necessary, stop data collection if the crystal was found to have moved significantly from its original position.

It has been established that the titanomaghemite specimen is primitive cubic; this means that many of the observed intensities are crystallographically equivalent. In the measurements reported here, one hemisphere of reciprocal space was examined; therefore reflections of the general form  $\{hkl\}$  contain 24 equivalents, whereas  $\{hk0\}$  and  $\{hhl\}$  reflections contain 12,  $\{hhh\}$  reflections contain

6,  $\{hhh\}$  reflections contain 4, and  $\{h00\}$  reflections contain only 3 equivalents. The original list of 3543 observed integrated intensities could therefore be collected into groups and reduced to 197 independent reflections by averaging the equivalents within a group.

Refinement of the structure parameters was carried out with the crystallographic least-squares program CRYLSQ. To begin with, only reflections with intermediate-range intensities were used so that approximate values for the scale factor could be found. Initial parameters for atom positions and anisotropic temperature factors were taken from those published by Tomas et al. (1983) for ordered  $LiFe_3O_8$ . This compound is found to have the same space group and a very similar arrangement of atoms to that of maghemite (Braun, 1952).

The least-squares refinement gave a very small extinction correction (or  $g$  factor) of  $0.05(1) \times 10^3$ . This result indicates that the arrangement of the mosaic blocks within the crystal is such as to approach that of the ideally imperfect crystal as described by Zachariassen (1967). The averaged intensities were then corrected for secondary extinction using the above  $g$  factor.

It was also necessary to employ a weighting scheme that downweights low-angle and strong reflections but allows more emphasis to be placed on the weak high-angle data that is more sensitive to atom positions. Atomic scattering factors for  $Fe^{2+}$ ,  $Fe^{3+}$ , and  $Ti^{4+}$  ions were taken from the *International Tables for X-Ray Crystallography* (1952), and those for  $O^{2-}$  from Tokonami (1965). Real and imaginary parts of the dispersion correction were taken from the *International Tables for X-Ray Crystallography* (1952). Absorption corrections applied were those given by Weber (1969) for spherical crystals. Least-squares refinements were repeated until optimized values had been found for scale, the seven atom positions, and 16 temperature factors (Tables 3 and 4).

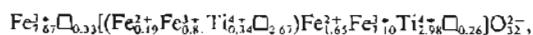
Under  $P4_32$  symmetry, two separate octahedral sites exist; these are represented in Table 3 by the symbols Fe(1) and Fe(3), with positions 12(d) and 4(b), respectively. The presence of three different types of cations ( $Fe^{2+}$ ,  $Fe^{3+}$ , and  $Ti^{4+}$ ) and cation vacancies on the two unique octahedral sites, along with the similarity in scattering factors for the three ions, meant that it was impossible to determine, with any degree of accuracy, the precise distribution of individual cations between these two octahedral sites.

In order to simplify this problem, it was necessary to make several assumptions, justifiable because the precise distribution of individual cations on each of the two octahedral sites does not have to be known to determine the overall symmetry of the specimen or the vacancy distribution between tetrahedral and octahedral sites. No peaks corresponding to tetrahedral  $Fe^{2+}$  were observed in the Mössbauer study, and the presence of  $Fe^{2+}$  and, in particular,  $Ti^{4+}$  on tetrahedral sites is unlikely. Thus, initially it was assumed that the tetrahedral sites were occupied by 8  $Fe^{3+}$  ions. The population parameter for this site was then refined and converged on a value of 0.96(2),

TABLE 3. Atom positions

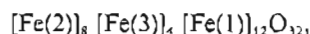
Atom	Position	x	y	z
Titanomaghemite specimen BM1929,1687, ( $a = 8.341 \pm 0.001 \text{ \AA}$ )				
Fe(1)	12(d)	0.12500	0.36623(6)	-0.11623(6)
Fe(2)	8(c)	-0.00444(6)	-0.00444(6)	-0.00444(6)
O(1)	8(c)	0.3862(3)	0.3862(3)	0.3862(3)
O(2)	24(e)	0.1179(3)	0.1304(3)	0.3837(3)
Fe(3)	4(b)	0.62500	0.62500	0.62500
Synthetic $\text{LiFe}_2\text{O}_4$ (Tomas et al., 1983)				
Fe(1)	12(d)	0.12500	0.36735(6)	-0.11735(6)
Fe(2)	8(c)	-0.00235(7)	-0.00235(7)	-0.00235(7)
O(1)	8(c)	0.3853(3)	0.3853(3)	0.3853(3)
O(2)	24(e)	0.1166(3)	0.1284(3)	0.3839(3)
Li(1)	4(b)	0.62500	0.62500	0.62500
Synthetic $\text{LiAl}_2\text{O}_4$ (Famery et al., 1979)				
Al(1)	12(d)	0.1250	0.3686(1)	-0.1186(1)
Al(2)	8(c)	-0.025(1)	-0.025(1)	-0.025(1)
O(1)	8(c)	0.3859(1)	0.3859(1)	0.3859(1)
O(2)	24(e)	0.1146(1)	0.1329(1)	0.3847(1)
Li(1)	4(b)	0.6250	0.6250	0.6250

indicating the presence of 4% tetrahedral vacancies, that is 7.67  $\text{Fe}^{2+}$  tetrahedral cations per unit cell, a value in very good agreement with that of 7.78 found in the Mössbauer work. The numbers of octahedral  $\text{Fe}^{2+}$ ,  $\text{Fe}^{3+}$ , and  $\text{Ti}^{4+}$  cations and cation vacancies were taken to be 1.84, 7.91, 3.32, and 2.93, respectively (the values found in the Mössbauer and microprobe studies). As a first approximation, it was assumed that 2.67 cation vacancies were present on the Fe(3) octahedral site. This is the number of cation vacancies present on this site in end-member maghemite and is therefore likely to be a reasonable initial value. The remaining 0.26 cation vacancies were assumed to be present on the Fe(1) octahedral site. We have already assumed Fe(1) to have 0.26 and Fe(3) to have 2.67 sites vacant; the remaining sites must therefore be occupied by  $\text{Fe}^{2+}$ ,  $\text{Fe}^{3+}$ , and  $\text{Ti}^{4+}$  ions. The 1.84  $\text{Fe}^{2+}$ , 7.91  $\text{Fe}^{3+}$ , and 3.32  $\text{Ti}^{4+}$  octahedral cations found in the Mössbauer and microprobe studies were therefore divided between the Fe(1) and Fe(3) sites in the ratio 11.74:1.33, where this ratio represents the numbers of each octahedral site occupied. The following structural formula results:

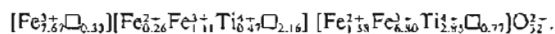


where  $\square$  represents a cation vacancy. Atomic scattering factors for each octahedral site were calculated on the basis of the above formula.

When the population parameter for the Fe(3) site was refined, the results obtained indicated that the cation distribution given in the above formula underestimated the scattering produced by this site by approximately 27%. This result meant that the number of cation vacancies on the Fe(3) site was less than the value of 2.67 assumed initially and that the number of cations was greater than the assumed value. Keeping the overall number of octahedral cations and vacancies constant (at the value found in the Mössbauer and microprobe studies), the numbers of  $\text{Fe}^{2+}$ ,  $\text{Fe}^{3+}$ , and  $\text{Ti}^{4+}$  ions on the Fe(3) site were increased by 27%, and those on the Fe(1) site were reduced by the appropriate amount, to account for the observed population parameters. The number of vacancies for the Fe(1) and Fe(3) sites were found by difference. The resulting general structural formula,



gives a formula for BM1929,1687 of



New atomic scattering factors for each octahedral site were then calculated on the basis of the new cation distribution predicted by the above formula. Refinement of the population parameters for each octahedral site indicated that the observed parameters agreed with those given by this above formula to within 2%. The population parameter for tetrahedral sites was found to agree within

TABLE 4. Anisotropic temperature factors ( $\times 10^3$ ) obtained for titanomaghemite specimen BM1929,1687

Atom	$\beta_{11}$	$\beta_{22}$	$\beta_{33}$	$\beta_{12}$	$\beta_{13}$	$\beta_{23}$
Fe(1)	335(9)	200(5)	200(5)	-28(5)	-28(5)	-77(7)
Fe(2)	183(3)	183(3)	183(3)	-3(5)	-3(5)	-3(5)
O(1)	203(18)	203(18)	203(18)	36(25)	36(25)	36(25)
O(2)	225(26)	535(33)	230(28)	-40(22)	24(20)	76(35)
Fe(3)	381(14)	381(14)	381(14)	8(16)	8(16)	8(16)

Note: Temperature factors are in the following form:

$$\exp[-(\beta_{11}h^2 + \beta_{22}k^2 + \beta_{33}l^2 + 2\beta_{12}hk + 2\beta_{13}hl + 2\beta_{23}kl)]$$

2% of that predicted by the Mössbauer and microprobe studies.

The arrangement of cations and cation vacancies on the two octahedral sites is similar to that observed in  $\text{LiAl}_2\text{O}_3$  by Famery et al. (1979), i.e., the octahedral positions 4(b) and 12(d) are occupied in a statistical manner. No evidence of ordering of cations or cation vacancies on the octahedral site, leading to a lower-symmetry space group, was found.

A complete list of observed and calculated structure factors obtained for the specimen under  $P4_332$  symmetry is given in Table 5.<sup>1</sup> Atom positions (Table 3) are found to be in good agreement with those found by Tomas et al. (1983) and Famery et al. (1979) for the compounds  $\text{LiFe}_2\text{O}_3$  and  $\text{LiAl}_2\text{O}_3$ , respectively, each of which crystallize with the same space group as this particular titanomaghemite specimen. Calculated bond lengths are shown in Table 6. The overall  $R$  factor found in the analysis was 2.35%, the weighted  $R$  factor was 2.50%, and the unit-cell parameter  $a = 8.341(1) \text{ \AA}$ .

## DISCUSSION

The single-crystal X-ray diffraction study of titanomaghemite described above shows that this sample has a primitive cubic Bravais lattice with the space group  $P4_332$ . Because this space group does not contain any symmetry operations involving inversion or reflection, it is possible for the crystals to exist in both right- and left-handed forms described by the space groups  $P4_332$  and  $P4_132$ —an enantiomorphous pair. Without resorting to precise measurements of Friedel-related pairs of reflections, it is impossible to distinguish between the two different forms of the structure (hence, in the above work, the space group  $P4_332$  was assumed for simplicity).

It is possible for the two enantiomorphous forms of such a structure to exist within an apparent single crystal as is found in  $\text{LiFe}_2\text{O}_3$  (van der Biest and Thomas, 1975). These two forms occur as small domains, the exact domain size being dependent upon sample history but generally of the order of  $0.1\text{-}\mu\text{m}$  diameter. Such a domain structure has been observed in dark-field electron micrographs of a natural maghemite crystal (Smith, 1979).

The X-ray and Mössbauer studies of titanomaghemite specimen BM1929,1687 also have enabled the cation and vacancy distributions to be determined. This observed distribution can be compared with the predictions of various models presented in the literature. According to Readman and O'Reilly (1971) the general formula for the cation distribution of any titanomaghemite is

$$\text{Fe}_{1-x}^{2+}\text{Fe}_x^{3+}[\text{Fe}_{(2-z+x)(1-x)}^{2+}\text{Fe}_{(1-x)(1-x)}^{3+}\text{Ti}_{(1-x)}^{4+}\square_{(1-x)}]O_4^{2-},$$

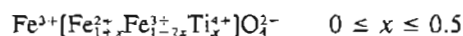
where  $x$  is the Fe/Ti ratio,  $z$  the degree of oxidation,  $R$  the spinel stoichiometry parameter, and  $\delta$  the number of

TABLE 6. Bond lengths calculated for titanomaghemite specimen BM1929,1687 under  $P4_332$  symmetry

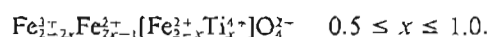
Bond	Distance (Å)
Fe(2)-O(2)	1.8789(2)
Fe(2)-O(1)	1.9038(2)
Fe(1)-O(2)	1.9581(2)
Fe(1)-O(2)	2.0209(2)
Fe(1)-O(1)	2.0870(2)
Fe(3)-O(2)	2.1327(3)
O(2)-O(2)	3.0641(3)
O(2)-O(1)	3.0928(3)
O(2)-O(2)	2.8672(3)
O(2)-O(2)	2.9198(3)
O(2)-O(2)	2.9678(3)
O(1)-O(2)	2.7265(3)
O(1)-O(2)	2.8722(3)
O(1)-O(1)	2.9549(3)
O(1)-O(2)	3.0928(3)

$\text{Fe}^{2+}$  ions on tetrahedral sites. This equation assumes that cation vacancies and  $\text{Ti}^{4+}$  ions are restricted to octahedral sites. Taking the structural formula established above BM1929,1687 and substituting values into the above equation yields  $x = 0.47(2)$ ,  $z = 0.82(2)$ ,  $R = 0.88(2)$ , and  $\delta = 0$ .

Since titanomaghemites form by the oxidation of titanomagnetites, it is possible to attempt to establish the composition of the parent titanomagnetite. Néel (1955) and Chevallier et al. (1955) proposed models for the cation distribution in titanomagnetites in which all the  $\text{Ti}^{4+}$  enters octahedral sites and  $\text{Fe}^{2+}$  first replaces  $\text{Fe}^{3+}$  in octahedral sites and only then  $\text{Fe}^{3+}$  in tetrahedral sites. This leads to the structural formulae



and



In this Néel-Chevallier model, no tetrahedral  $\text{Fe}^{2+}$  exists in the parent titanomagnetite for  $x < 0.5$ . It has been established that  $x = 0.47(2)$  in BM1927,1687, and this value also applies to the titanomagnetite parent. The above model therefore stipulates that no tetrahedral  $\text{Fe}^{2+}$  should occur in either the parent titanomagnetite or the titanomaghemite, as observed experimentally. Substituting values for  $x$  into the above formula gives

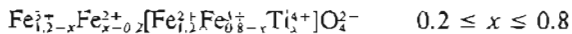
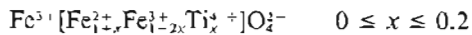


for the parent titanomagnetite composition.

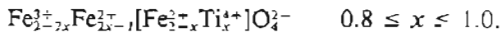
Because of poor correspondence with certain of the physical properties of titanomagnetites, an alternative to the Néel-Chevallier model was proposed by O'Reilly and Banerjee (1965). In the O'Reilly-Banerjee model, which shows better agreement with titanomagnetite properties,  $\text{Fe}^{2+}$  begins to occupy the tetrahedral sites at  $x > 0.2$ . The model is similar to the Néel-Chevallier model over the compositional ranges  $0 < x < 0.2$  and  $0.8 < x < 1.0$  but varies continuously over  $0.2 < x < 0.8$  with no dis-

<sup>1</sup> A copy of Table 5 may be ordered as Document AM-88-364 from the Business Office, Mineralogical Society of America, 1625 I Street, N.W., Suite 414, Washington, D.C. 20006, U.S.A. Please remit \$5.00 in advance for the microfiche.

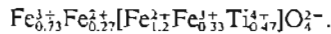
continuities at  $x = 0.5$ . The following structure formulae result:



and



Assuming the O'Reilly-Banerjee model, the following structural formula results for the parent titanomagnetite of BM1929,1687:



The presence of  $\text{Fe}^{2+}$  in tetrahedral sites in the parent titanomagnetite strongly suggests that  $\text{Fe}^{2+}$  in tetrahedral sites should also occur in the titanomaghemite, but this was not observed experimentally. It is possible that all of the tetrahedral-site  $\text{Fe}^{2+}$  has been oxidized during "maghemitization," but this seems unlikely with a significant proportion of octahedral  $\text{Fe}^{2+}$  still present in the sample studied. The Néel-Chevallier model therefore appears to give a more plausible description of the parent titanomagnetite in this case.

The presence of tetrahedral-site vacancies, although not specifically taken into account in the model titanomaghemite formula of Readman and O'Reilly (1971) was not ruled out by them. They noted that during oxidation of the parent titanomagnetite, octahedral-site  $\text{Fe}^{2+}$  diffuses to the crystal surface where it is oxidized by adsorbed oxygen ions forming new tetrahedral and octahedral sites. The majority of these vacancies are then filled by diffusing  $\text{Fe}^{3+}$  ions, but for high degrees of oxidation, some tetrahedral sites will remain vacant.

#### ACKNOWLEDGMENTS

The Natural Environment Research Council is thanked for supporting this research through a studentship to S.C. The British Museum (Natural History) and Dr. C. J. Stanley, in particular, and Dr. G. D. Price (University College, London) are thanked for providing specimens for study. Mr. L. W. Becker (AERE, Harwell) is thanked for help with the low-temperature Mössbauer measurements, and Christine Gee and Beverley Parker are thanked for help in preparation of the manuscript.

#### REFERENCES CITED

- Armstrong, R.J., Morrish, A.H., and Sawatzky, G.A. (1966) Mössbauer study of ferric ions in a spinel. *Physics Letters*, 23, 414-416.
- Bauminger, R., Cohen, S.C., Marinov, A., Ofer, S., and Segal, E. (1961) Study of the low-temperature transition in magnetite and the internal fields acting on iron nuclei in some spinel ferrites, using Mössbauer absorption. *Physical Review*, 122, 1447-1450.
- Bond, W.L. (1951) Making small spheres. *Review of Scientific Instruments*, 22, 344-345.
- Braun, P. (1952) A superstructure in spinels. *Nature*, 170, 1123.
- Chevallier, R.J., Bolfa, J., and Mathieu, S. (1955) Titanomagnetites et iménites ferromagnétiques (I). *Étude optique, radiocristallographique,*

- chimique. Bulletin de Société française de Minéralogie et Cristallographie*, 78, 307-346.
- Coccy, J.M.D., Morrish, A.H. and Sawatzky, G.A. (1971) Mössbauer study of conduction in magnetite. *Journal de Physique (Paris) Colloquium*, 32, C271-C273.
- Cormack, A.N., and Price, G.D. (1985) Vacancy ordering of maghemite. In L.C. Dufour, Ed. *Reactivity of solids*. Elsevier, New York.
- Craig, J.R., and Vaughan, D.J. (1981) *Ore microscopy and ore petrography*. Wiley-Interscience, New York.
- Famery, R., Queyroux, F., and Gilles, J.C. (1979) Etude structurale de la forme ordonnée de  $\text{LiAl}_2\text{O}_4$ . *Journal of Solid State Chemistry*, 30, 257-263.
- Greaves, C. (1983) A powder neutron diffraction investigation of vacancy and covalence in  $\gamma$ -ferric oxide. *Journal of Solid State Chemistry*, 49, 325-333.
- International tables for X-ray crystallography, vol. IV (1952) N.F.M. Henry and K. Lonsdale, Eds. Kynoch Press, Birmingham, England.
- Ishikawa, Y., Sato, S., and Syono, Y. (1971) Neutron and magnetic studies of a single crystal of  $\text{Fe}_2\text{TiO}_4$ . *Journal of the Physical Society of Japan*, 31, 452-460.
- Kelly, W.H., Folen, V.J., Hass, M., Schreyer, W.N., and Beard, G.B. (1961) Magnetic field at the nucleus in spinel-type crystals. *Physical Review*, 124, 80-86.
- Longworth, G. (1984) Spectral data reduction and refinement. In G.L. Long, Ed., *Mössbauer spectroscopy applied to inorganic chemistry*, vol. 1. Plenum, New York.
- Néel, L. (1955) Some theoretical aspects of rock magnetism. *Advances in Physics*, 4, 191-243.
- O'Reilly, W., and Banerjee, S.K. (1965) Cation distribution in titanomagnetites  $(1-x)\text{Fe}_2\text{O}_3 \cdot x\text{Fe}_2\text{TiO}_4$ . *Physics Letters*, 17, 237-238.
- Readman, P.W., and O'Reilly, W. (1971) Oxidation processes in titanomagnetites. *Zeitschrift für Geophysik*, 37, 329-338.
- Sawatzky, G.A., van der Woude, F., and Morrish, A.H. (1969) Mössbauer study of several ferromagnetic spinels. *Physical Review*, 187, 747-757.
- Smith, P.P.K. (1979) The observation of enantiomorphous domains in a natural maghemite. *Contributions to Mineralogy and Petrology*, 69, 249-254.
- Sosman, R.B., and Posnjak, E. (1925) Ferromagnetic ferric oxide, artificial and natural. *Journal of the Washington Academy of Science*, 15, 329-342.
- Stephenson, A. (1969) The temperature dependent cation distribution in titanomagnetites. *Geophysical Journal of the Royal Astronomical Society*, 18, 199-210.
- Stewart, J.M., Kruger, G.J., Amman, H.L., Dickinson, C., and Hall, S.R. (1974) X-ray 74. University of Maryland, College Park, Maryland.
- Sweatman, T.R., and Long, J.V.P. (1969) Quantitative electron-probe microanalysis of rock-forming minerals. *Journal of Petrology*, 10, 332-379.
- Tokonami, M. (1965) Atomic scattering factor for  $\text{O}^{2-}$ . *Acta Crystallographica*, 19, 486.
- Tomas, A., Laruelle, P., Dormann, J.L., and Nogués, M. (1983) Affinement de la structure des formes ordonnées et désordonnées de l'octaoxopentaferrate de lithium,  $\text{LiFe}_5\text{O}_8$ . *Acta Crystallographica*, C39, 1615-1617.
- van der Biest, O., and Thomas, G. (1975) Identification of enantiomorphism in crystals by electron microscopy. *Acta Crystallographica*, A31, 70-76.
- Weber, von K. (1969) Eine neue absorptionsfaktortafel für kugelförmige proben. *Acta Crystallographica*, B25, 1174-1178.
- Zachariasen, W.H. (1967) A general theory of X-ray diffraction in crystals. *Acta Crystallographica*, 23, 558-564.

MANUSCRIPT RECEIVED DECEMBER 31, 1986

MANUSCRIPT ACCEPTED SEPTEMBER 22, 1987